Applied Physics Letters

Reaction-diffusion analysis for one-step plasma etching and bonding of microfluidic devices

Cite as: Appl. Phys. Lett. **98**, 174102 (2011); https://doi.org/10.1063/1.3578450
Submitted: 14 February 2011 . Accepted: 23 March 2011 . Published Online: 25 April 2011

Michel Rosso, Volkert van Steijn, Louis C. P. M. de Smet, Ernst J. R. Sudhölter, Chris R. Kleijn, and Michiel T. Kreutzer

Reaction-diffusion analysis for one-step plasma etching and bonding of microfluidic devices

Michel Rosso,[1,2] Volkert van Steijn,[1] Louis C. P. M. de Smet,[1] Ernst J. R. Sudhölter,[1] Chris R. Kleijn,[2] and Michiel T. Kreutzer[1,a)]
[1]*Chemical Engineering, Delft University of Technology, Julianalaan 136, 2628 BL Delft, The Netherlands*
[2]*Multiscale Physics, Delft University of Technology, Prins Bernhardlaan 6, 2628 BW Delft, The Netherlands*

(Received 14 February 2011; accepted 23 March 2011; published online 25 April 2011)

A self-similar reaction front develops in reactive ion etching when the ions penetrate channels of shallow height h. This relates to the patterning of microchannels using a single-step etching and bonding, as described by Rhee *et al.* [Lab Chip **5**, 102 (2005)]. Experimentally, we report that the front location scales as $x_f \sim ht^{1/2}$ and the width is time-invariant and scales as $\delta \sim h$. Mean-field reaction-diffusion theory and Knudsen diffusion give a semiquantitative understanding of these observations and allow optimization of etching times in relation to bonding requirements. © *2011 American Institute of Physics*. [doi:10.1063/1.3578450]

The use of microfluidic devices in bioanalytical techniques often requires the ability to form patterns of biomolecules on microchannel walls.[1] One typically patterns a flat surface, for instance, using spotting, electrospraying, or jet printing[2] before clamping a microfluidic network on top. Sealing this network irreversibly to form a device is a challenge, as most sealing processes, most prominently plasma-activated bonding, destroy the deposited pattern. A clever trick introduced by Khademhosseini *et al.*[3] combines microstamping and bonding. Leaving the stamp in place during plasma exposure ensures a faithful transfer of material from the stamp to the contacted surface while the surrounding surface is activated for bonding. An air plasma can also be used to etch patterns by destroying organic coatings[4] or polymer surfaces[5] in regions not in conformal contact with a polydimethylsiloxane (PDMS) mask [Figs. 1(a)–1(c)]. At the same time, silicon-based surfaces (e.g., Si, SiO_2, PDMS) are activated such that an irreversible seal is created, when it is pressed onto a similarly plasma-exposed microchannel network [Fig. 1(d)].

This single-step etch-activate-bond method, introduced by Rhee *et al.*,[6] raises the important practical question how much time is needed to etch a surface partially protected by a mask, particularly because the optimal plasma exposure for bonding has a narrow range.[7] Rhee *et al.* extensively explored the parameter space involved for their particular equipment and masks. They found that the height of the features, in addition to mask and pattern size, was important, giving optimum etching times from 1 to 10 min, but no general model or physically sound recipe was presented.

In this letter, we analyze how a reaction-diffusion model predicts the progression of the plasma front under the mask to produce 10–100 μm patterns on centimeter-scale surfaces. Our understanding shows how the progress of the front critically depends on the height of the free space under the mask, and we provide an experimentally validated order-of-magnitude estimate for the diffusive penetration based on conditions in the plasma chamber.

The patterns were produced on glass surfaces coated with bovine serum albumin (BSA) tagged with biotin. A soft PDMS mask, including the desired protruding features, was placed on the glass surface [Fig. 1(a)]. The masked surface was then exposed to a cold ($T \sim 300$ K) air-based plasma (Harrick PDC-002) at $p \sim 0.2$ mbar [Fig. 1(b)]. The plasma penetrated under the mask and reacted with the unprotected coating. After removal of the mask, a second slab of PDMS, featuring the microchannel network and activated in the same plasma, is aligned by eye on the patterned surface [Fig. 1(c)] and pressed to seal the device [Fig. 1(d)].

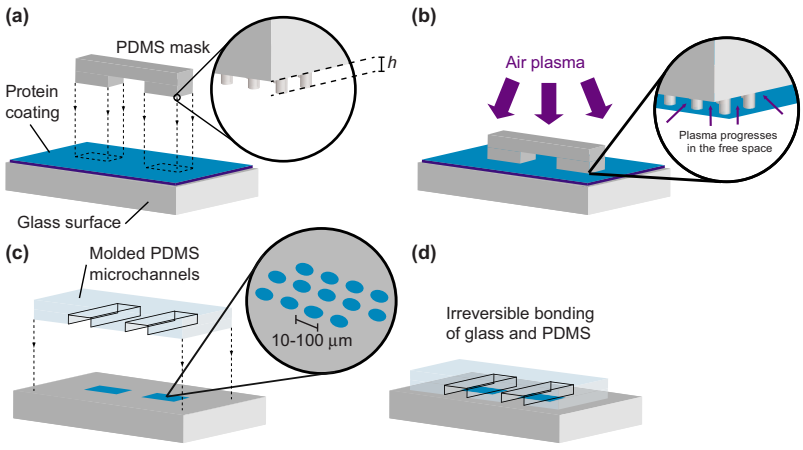

FIG. 1. (Color online) Fabrication steps: (a) placing a PDMS mask with protruding features of height h onto a flat glass surface coated with a layer of protein, (b) Plasma treatment to destroy the coating, where it is not in conformal contact with the mask and to activate the bare surface regions, (c) Removal of the mask reveals the created patterns, (d) Irreversibly sealing a plasma-treated microchannel network on top.

a)Electronic mail: m.t.kreutzer@tudelft.nl.

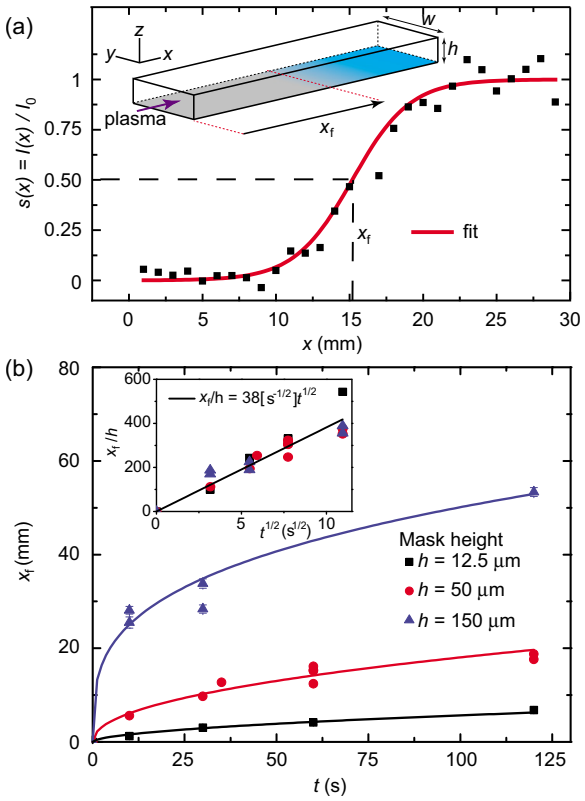

FIG. 2. (Color online) (a) Normalized fluorescence intensity $s(x)$ along a channel of width w and height h (see inset) after plasma patterning ($h=50$ μm, $t=60$ s). (b) The location of the front x_f, at $s(x_f)=1/2$, vs time for different channel heights with fitted curves $x_f \sim \sqrt{t}$. Inset: master curve $x_f \sim h\sqrt{t}$.

First, we used masks featuring a straight microchannel of different heights h and width w ($w \gg h$) with an entrance at one side [Fig. 2(a), inset]. After etching the coated surface for a time t, with the microchannel on top of it, we visualized the progress of the etching into the channel by incubating the surface with fluorescently labeled streptavidin and washing it with a buffer solution. The streptavidin binds with high specificity to biotin in the unetched coating and washes readily from the etched, uncoated surface. The now fluorescently labeled coating allowed a direct measurement of the surface concentration $S(x)$ of reactive sites per unit area under a fluorescence microscope. We recorded the cross-sectional average intensity $I(x)=\int_0^w I(x,y)dy$ as a function of x, the distance from the entrance. The fluorescence I_0 on a protected patch of coating was used to normalize the intensity and to define the dimensionless surface concentration as a fraction of the unetched surface concentration S_0, using $s(x)=S(x)/S_0=I(x)/I_0$.

Figure 2(a) depicts a normalized intensity profile in a typical experiment, clearly showing a reaction zone centered at $x_f=15$ mm ($s=1/2$) between a region, where the coating is etched away ($x<10$ mm, $s\approx 0$) and a region, where the coating is intact ($x>22$ mm, $s\approx 1$). The fractional coverage $s(x)$ evolves in a self-similar fashion, well described by $s(x)=(1/2)(1+\mathrm{erf}\ \eta)$, where $\eta=(x-x_f)/\delta$ is a similarity variable that captures the evolution of the location of the front $x_f(t)$ and the width of the front $\delta(t)$. The fact that we have a narrow front shows that the etching is limited by diffusion to the front, after an initial phase. Mean-field models for reaction and diffusion, introduced by Gálfi and Racz,[8] predict asymptotic (long-time) behavior of x_f and δ. Briefly, reaction is mostly confined to a length that scales as δ, balanced by diffusion over a depletion length with negligible reaction that scales as x_f. Typically, the scalings for x_f and δ are different.

Before we discuss the asymptotic behavior of η, we notice that mean path length λ of the plasma ions is much larger than the channel height. Diffusion, then, is dominated by wall collisions. For a channel of length L, allowing for lengthwise variations in cross-sectional area A and perimeter o, the pseudo-one-dimensional Knudsen[9] diffusion coefficient $D=(1/3)Gv$ depends on the channel geometry as $G=4L(\int_L o/Adx)^{-1}$, or, for rectangular channels with $h \ll w$ and the ion speed v from kinetic gas theory, $D=(2/3)h(8k_BT/\pi m)^{1/2}$. The fact that, unlike molecular diffusion at higher pressures, D scales with h for rarefied conditions has important consequences for all scaling relations that we discuss below.

Provided that we use this height-dependent diffusion coefficient, our profiles are in agreement with similarity solutions[10] for reaction-diffusion problems. Our system is one in which the ions diffuse but the surface coating molecules do not. For arbitrary kinetics $R=kC^aS^b$, the plasma ion concentration C and surface concentration S obey

$$h\partial_t C = hD\partial_{xx}C - kC^aS^b, \tag{1}$$

$$\partial_t S = -kC^aS^b. \tag{2}$$

Using the coordinate stretching transformation in a moving reference frame $\eta=(x-\nu t^\sigma)/t^\alpha$, we start with $x_f=\nu t^\sigma$, the asymptotic scaling for the front location using the so-called Stefan moving boundary condition, originally introduced for ice-layer growth.[11] The speed of the front is expressed as the number of ions needed to etch an area per unit time, which balances the flux of ions to the front, or $S_0\partial_t x_f = hD\partial_x C(0)$. The concentration of ions at the entrance is kept at C_0, and $\partial_x C \sim C_0/x_f$ because the concentration of ions is much smaller in the reaction zone. Then, after some algebra,

$$x_f = \nu t^{1/2}, \quad \nu = 2h\left(\frac{C_0^2}{S_0^2}\frac{8k_BT}{\pi m}\right)^{1/4}. \tag{3}$$

Experimentally, we found that the position of the reaction front progressed as $x_f=38ht^{1/2}$ [inset of Fig. 2(b)], in agreement with estimates of the proportionality factor in Eq. (3), $\nu/h=5\times 10^1$ $s^{-1/2}$, based on $S_0\sim(1\ \mathrm{nm}^2)^{-1}=10^{18}$ m^{-2} and $C_0\sim 10^{-4}p/RT\sim 10^{18}$ m^{-3} for our system. It is surprising that, apparently, a single ion can etch 1 nm^2 of a dense BSA monolayer coating, although this can be rationalized by a radical-initiated propagation mechanism that breaks the BSA into volatile fragments. We note that the etching times reported by Rhee *et al.*[6] for a different coating (poly-L-lysine) but similar plasma conditions are in perfect agreement with Eq. (3) with a slightly different constant $\nu/h=3\times 10^1$ $s^{-1/2}$.

Fully resolving the concentrations inside the reaction zone is only possible when the reaction kinetics are known in detail.[12] Here we assume $a=b=1$ in Eqs. (1) and (2), and find the scaling of δ as follows. The observed self-similar profiles suggest for the reaction zone (of width $\delta\sim t^\alpha$) the ansatz $S\sim t^0\Xi(\eta)$ while $C\sim t^{-\gamma}\Phi(\eta)$ and $R\sim t^{-\beta}\Psi(\eta)$ can have time-dependent scalings ($\Phi(\eta)$, $\Xi(\eta)$ and $\Psi(\eta)$ represent the time-invariant parts). First, self-similarity requires that the flux $hDC_0/\nu t^{1/2}$ balances the reaction rate kC_fS at all

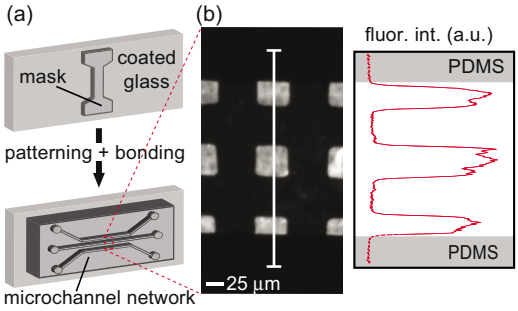

FIG. 3. (Color online) Fluorescence patterns inside irreversibly sealed microfluidic channels: (a) a mask is used to form patterns in three adjacent channels, (b) fluorescence patterns obtained after incubation with fluorescent streptavidin, and profile of fluorescence intensity along the indicated line.

times, which gives the scale of C in the reaction zone, $C_f/C_0 \sim (hD/\nu k S_0)t^{-1/2}$, i.e., $\gamma = 1/2$. Second, the reaction zone is so narrow that it equilibrates quickly with the change in ion flux to it, so reaction and diffusion balance everywhere in the reaction zone. Then, scaling the second derivative of C as $\partial_{xx}C \sim C_f/\delta^2$ implies that $hDC_f/\delta^2 \sim kC_f S_0$, from which one not only finds that the front width is time-invariant ($\alpha = 0$), but also the scaling

$$\delta \sim h\left(\frac{k_B T}{k^2 S_0^2 m}\right)^{1/4}, \tag{4}$$

which agrees with our observation that $\delta \sim t^0$. Experimentally, δ scales with h as $\delta = 8 \times 10^1 h$, which can be combined with the earlier estimate of S_0 to estimate the reaction rate constant as $k \sim 10^5$ $m^3/(mol\ s)$. Finally, balancing the integral of the rate ($\sim \delta R$) with the flux to the zone $hDC_0/\nu t^{1/2}$, we find that $\alpha - \beta = -1/2$, or, with $\alpha = 0$, that the rate of reaction slows down asymptotically as $R \sim t^{-1/2}$. In summary, the rate slows down as fast as the flux and the width does not grow when $a = 1$, and $R/C_f = kS$ is constant in the reaction zone because S remains of the same scale throughout.

We have, up to now, only reported fluorescence intensities for glass surfaces without microchannel networks bonded on top. Moreover, in the above the channel did not have features to mask small spots of coating. Such features do not change our analysis as long as $h \ll \lambda$ and $D \propto h$, i.e., as long as h is by far the shortest distance under the mask. Figure 3 shows intensities of fluorescently labeled patterns, after bonding, in a channel that was patterned with micron-sized features and activated for bonding using a single mask. These mask patterns were accurately reproduced inside the closed microchannels with a spatial resolution predominantly depending on the accuracy of fabrication of the features on the mask (~ 1 μm).

A remaining question is whether the absence of fluorescence is sufficient proof that the surface has been etched completely. Indeed, $s \approx 0$ in Fig. 2 only shows that the biotin-tagged BSA is too damaged by radicals to bind streptavidin, but not necessarily that it is completely etched away. We examined how clean the surfaces were after plasma treatment with space-resolved attenuated total reflection-fourier transform infrared (ATR-FTIR) spectroscopy. In these experiments ATR crystals (ZnSe) were coated with biotin-tagged BSA and covered with single channel PDMS masks like those used for Fig. 2. After plasma treatment and removal of the PDMS, the crystal was scanned in the FTIR spectrophotometer. The ATR-FTIR spectra, obtained by scanning lines of 11 reflections in the direction of the etched channel with 1 mm steps, had strongly (85%) reduced CH_2/CH_3 stretching vibrations (at 2957, 2925 and 2850 ± 2 cm^{-1}) typical for organic material (biotin and proteins) in the etched regions, indicating that very little residual organic material remains.

Finally, using the results of this letter, it is possible to optimize the plasma time. Normally, one would optimize for bonding strength, which has an optimum because underexposure leads to under-activation while over-exposure leads to a reduction in activated surface groups by back-biting reactions and cracking.[7] In general, this optimum need not agree with the minimal time needed to etch. The results here can, within limits, be used to select the mask height, to accomplish both bonding and etching. The quality of our bonding is characterized by a delamination pressure of 1 bar, one quarter of what can be achieved for PDMS-glass devices[7] from clean glass, but good enough for most uses.

In conclusion, we elucidate the relevant physics for combined patterning and bonding using a single processing step of masked surfaces. In particular, we show how geometry of the channel is taken into account for rarefied gas diffusion, which introduces an additional height dependence. Using mean-field reaction diffusion models, we show that the reaction front propagates according to $x_f \propto ht^{1/2}$, having a time-invariant width $\delta \propto h$, which allows the optimization of etching times together with other process requirements. Accurate orders of magnitude for all scaling variables were based on reasonable estimates of the conditions in the plasma chamber. The insights presented herein can be generally applied to reactive etching in small ducts and plasma patterning of silicon-based surfaces with different types of thin coatings.

This research was supported by the Delft Centre for Sustainable Industrial Processes (DCSIP) and by VENI Grant Nos 700.56.404 and 700.56.412 from the Netherlands Organization for Scientific Research (NWO) to MTK and LCP-MdS.

[1] A. Folch and M. Toner, Annu. Rev. Biomed. Eng. **2**, 227 (2000); J. El-Ali, P. K. Sorger, and K. F. Jensen, Nature (London) **442**, 403 (2006).
[2] M. Schena, D. Shalon, R. W. Davis, and P. O. Brown, Science **270**, 467 (1995); J. J. Diaz-Mochón, G. Tourniaire, and M. Bradley, Chem. Soc. Rev. **36**, 449 (2007); J.-U. Park, M. Hardy, S. J. Kang, K. Barton, K. Adair, D. Mukhopadhyay, C. Lee, M. Strano, A. Alleyne, J. Georgiadis, P. Ferreira, and J. Rogers, Nature Mater. **6**, 782 (2007).
[3] A. Khademhosseini, K. Y. Suh, S. Jon, G. Eng, J. Yeh, G. J. Chen, and R. Langer, Anal. Chem. **76**, 3675 (2004).
[4] C. Y. Xue and K. L. Yang, Langmuir **23**, 5831 (2007); M. Rosso, M. Giesbers, C. G. P. H. Schroen, and H. Zuilhof, *ibid.* **26**, 866 (2010).
[5] J. P. Frimat, H. Menne, A. Michels, S. Kittel, R. Kettler, S. Borgmann, J. Franzke, and J. West, Anal. Bioanal. Chem. **395**, 601 (2009); A. Tourovskaia, T. Barber, B. T. Wickes, D. Hirdes, B. Grin, D. G. Castner, K. E. Healy, and A. Folch, Langmuir **19**, 4754 (2003); B. A. Langowski and K. E. Uhrich, *ibid.* **21**, 10509 (2005).
[6] S. W. Rhee, A. M. Taylor, C. H. Tu, D. H. Cribbs, C. W. Cotman, and N. L. Jeon, Lab Chip **5**, 102 (2005).
[7] S. Bhattacharya, A. Datta, J. M. Berg, and S. Gangopadhyay, J. Microelectromech. Syst. **14**, 590 (2005).
[8] L. Gálfi and Z. Racz, Phys. Rev. A **38**, 3151 (1988).
[9] M. Knudsen, Ann. Phys. **333**, 75 (1909); S. Gruener and P. Huber, Phys. Rev. Lett. **100**, 064502 (2008).
[10] Z. Jiang and C. Ebner, Phys. Rev. A **42**, 7483 (1990); C. Léger, F. Argoul, and M. Z. Bazant, J. Phys. Chem. B **103**, 5841 (1999); Z. Koza, Physica A **240**, 622 (1997).
[11] J. Stefan, Ann. Phys. **278**, 269 (1891).
[12] M. Z. Bazant and H. A. Stone, Physica D **147**, 95 (2000).